Pyrimidin-2(1H)-ones based inhibitors of Mycobacterium tuberculosis orotate phosphoribosyltransferase

ARTICLE *in* EUROPEAN JOURNAL OF MEDICINAL CHEMISTRY · APRIL 2012

Impact Factor: 3.45 · DOI: 10.1016/j.ejmech.2012.04.031 · Source: PubMed

European Journal of Medicinal Chemistry 54 (2012) 113–122

Contents lists available at SciVerse ScienceDirect

European Journal of Medicinal Chemistry

journal homepage: http://www.elsevier.com/locate/ejmech

Original article

Pyrimidin-2(1*H*)-ones based inhibitors of *Mycobacterium tuberculosis* orotate phosphoribosyltransferase

Ardala Breda [a,b,c], Pablo Machado [a,b,c], Leonardo Astolfi Rosado [a,b,d], André Arigony Souto [c,e], Diógenes Santiago Santos [a,b,c], Luiz Augusto Basso [a,b,c,*]

[a] *Instituto Nacional de Ciência e Tecnologia em Tuberculose, Pontifícia Universidade Católica do Rio Grande do Sul, Avenida Ipiranga 6900, Prédio 92A – TECNOPUC, 90619-900 Porto Alegre, Rio Grande do Sul, Brazil*

[b] *Centro de Pesquisas em Biologia Molecular e Funcional, Pontifícia Universidade Católica do Rio Grande do Sul, Avenida Ipiranga 6900, Prédio 92A – TECNOPUC, 90619-900 Porto Alegre, Rio Grande do Sul, Brazil*

[c] *Programa de Pós-Graduação em Biologia Celular e Molecular, Pontifícia Universidade Católica do Rio Grande do Sul, Avenida Ipiranga 6900, Prédio 92A – TECNOPUC, 90619-900 Porto Alegre, Rio Grande do Sul, Brazil*

[d] *Programa de Pós-Graduação em Medicina e Ciências da Saúde, Pontifícia Universidade Católica do Rio Grande do Sul, Avenida Ipiranga 6900, Prédio 92A – TECNOPUC, 90619-900 Porto Alegre, Rio Grande do Sul, Brazil*

[e] *Faculdade de Química, Pontifícia Universidade Católica do Rio Grande do Sul, Avenida Ipiranga 6900, Prédio 92A – TECNOPUC, 90619-900 Porto Alegre, Rio Grande do Sul, Brazil*

HIGHLIGHTS

- Selection and optimization of inhibitors based on *Mt*OPRT kinetic mechanism.
- Identification of *Mt*OPRT inhibitors with nanomolar inhibition constant values.
- *In vitro* kinetic assays to characterize binding mode of inhibitors.
- Thermodynamic discrimination profiles of inhibitors assessed by ITC.
- Inhibitory activity of **13** is likely due to entropy optimization.

GRAPHICAL ABSTRACT

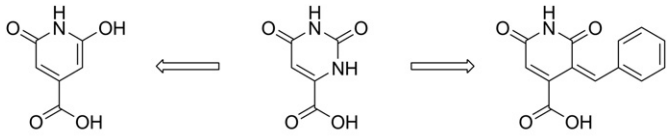

ARTICLE INFO

Article history:
Received 27 October 2011
Received in revised form
20 April 2012
Accepted 24 April 2012
Available online 30 April 2012

Keywords:
Mycobacterium tuberculosis
Tuberculosis
Pyrimidine
Orotate phosphoribosyltransferase

ABSTRACT

Tuberculosis (TB) is an ancient human chronic infectious disease caused mainly by *Mycobacterium tuberculosis*. The emergence of strains resistant to first and second line anti-TB drugs, associated with the increasing number of TB cases among HIV positive subjects, and the large number of individuals infected with latent bacilli have urged the development of new strategies to treat TB. Enzymes of nucleotide metabolism pathways provide promising molecular targets for the development of drugs, aiming at both active and latent TB. The orotate phosphoribosyltransferase (OPRT) enzyme catalyzes the synthesis of orotidine 5′-monophosphate from 5′-phospho-α-D-ribose 1′-diphosphate and orotic acid, in the *de novo* pyrimidine synthesis pathway. Based on the kinetic mechanism and molecular properties, here we describe the design, selection and synthesis of substrate analogs with inhibitory activity of *M. tuberculosis* OPRT (*Mt*OPRT) enzyme. Steady-state kinetic measurements were employed to determine the mode of inhibition of commercially available and chemically derived compounds.

Abbreviations: TB, tuberculosis; MTB, *Mycobacterium tuberculosis*; OPRT, orotate phosphoribosyltransferase; OA, orotate; PRPP, α-D-5-phosphoribosyl-1-pyrophosphate; K_m, Michaelis–Menten constant; OMP, orotidine 5′-monophosphate; PP_i, pyrophosphate; UMP, uridine 5′-monophosphate; *Mt*OPRT, *M. tuberculosis*' OPRT; FTIR, Fourier transform infrared; ITC, isothermal titration calorimetry; UATR, universal attenuated total reflectance.

* Corresponding author. Instituto Nacional de Ciência e Tecnologia em Tuberculose, Pontifícia Universidade Católica do Rio Grande do Sul, Avenida Ipiranga 6900, Prédio 92A – TECNOPUC, 90619-900 Porto Alegre, RS, Brazil. Tel./fax: +55 51 3320 3629.

E-mail addresses: ardalabreda@gmail.com (A. Breda), pablomachado.mail@gmail.com (P. Machado), leo.rosado@gmail.com (L.A. Rosado), arigony@pucrs.br (A.A. Souto), diogenes@pucrs.br (D.S. Santos), luiz.basso@pucrs.br (L.A. Basso).

0223-5234/$ – see front matter
doi:10.1016/j.ejmech.2012.04.031

Inhibitors
Pyrimidin-2(1*H*)-ones compounds

The 6-Hydroxy-2-oxo-1,2-dihydropyridine-4-carboxylic acid (**6**) chemical compound and its derivative, 3-Benzylidene-2,6-dioxo-1,2,3,6-tetrahydropyridine-4-carboxylic acid (**13**), showed enzyme inhibition constants in the submicromolar range. Isothermal titration calorimetry data indicated that binding of both compounds to *Mt*OPRT have negative enthalpy and favorable Gibbs free energy probably due to their high complementarity to the enzyme's binding pocket. Improvement of compound **13** hydrophobic character by addition of an aromatic ring substituent resulted in entropic optimization, reflected on a thermodynamic discrimination profile characteristic of high affinity ligands. These inhibitors represent lead compounds for further development of *Mt*OPRT inhibitors with increased potency, which may be tested as anti-TB agents.

1. Introduction

Tuberculosis (TB) is an ancient human chronic infectious disease [1], caused mainly by *Mycobacterium tuberculosis* (MTB) [2]. TB has been responsible for the death of over 2 million people annually, and in 2009 there were an estimated 26 deaths per 100 000 population [3].

TB treatment regimen includes six month therapy with rifampicin and isoniazid, supplemented with pyrazinamide and ethambutol in the first two months [3,4]. The poor compliance to the current treatment, owing to its length and side-effects [5], along with HIV infection emergence, leads to the occurrence of multi drug-resistant and extensively drug-resistant TB strains [3], for which the standard treatment shows no bactericidal and sterilizing activity [4,6]. Recently, a totally resistant strain, denoted as TDR-TB, has been described as resistant to all first and second line classes of anti-TB drugs tested [7,8]. Currently anti-TB available drugs are considered not completely efficacious [5] due to natural disease characteristics and emerging resistant strains that might impose some obstacles to its treatment [4]. Thus, novel TB treatments should be active against drug-resistant strains, and, ideally, be able to eliminate latent forms of TB [9]. Latent TB represents a significant infection reservoir, since almost 32% of world population is positive on tuberculin purified protein derivative skin test [3].

The nucleotide metabolism is an essential pathway for microorganism viability [10], including MTB and the vaccinal strain *Mycobacterium bovis* BCG [11]. In addition, *de novo* pyrimidine biosynthesis has already been shown to be required for cell invasion and virulence of obligatory parasites [12,13], in which disruption of this pathway leads to avirulent pyrimidine auxotrophs [12]. Although the metabolism required for sustaining mycobacterial survival during TB latency is still poorly understood, experimental evidence points to the maintenance of nucleotide synthesis in latent bacillus [14]. A specific inhibitor that targets a nucleotide synthesis enzyme has thus the potential of being effective against both active and latent TB.

Orotate phosphoribosyltransferase (OPRT, EC 2.4.2.10) catalyzes the fifth reaction in the *de novo* synthesis of pyrimidine nucleotides, converting orotate (OA) and α-D-5-phosphoribosyl-1-pyrophosphate (PRPP) to orotidine 5′-monophosphate (OMP), and pyrophosphate (PP_i), in the presence of Mg^{2+} (Fig. 1A). OMP is further decarboxylated into UMP, ultimately leading to DNA and RNA synthesis. OPRT homologs have been explored as targets for the development of inhibitors to treat malaria [13,15–17] and toxoplasmosis [18], as well as to cancer treatment for its role in 5-fluoruracil metabolism [19,20]. *Salmonella typhimurium* OPRT inhibitors have also been described [21].

Molecular, kinetic and thermodynamic characterization of *Mt*OPRT have recently been described [22]. *Mt*OPRT follows a Mono–Iso Ordered Bi Bi kinetic mechanism (Fig. 1B). Determination of *Mt*OPRT kinetic parameters and enzyme mechanism allowed the selection and testing of several commercially available compounds that might act as specific inhibitors of this mycobacterial enzyme (Fig. 2 and Table 1 – Compounds **1**–**8**). Starting compound selection was based on molecular similarity to *Mt*OPRT substrate OA. The rationale for choosing OA analogs is as follows: PRPP *Mt*OPRT substrate is also substrate for several other metabolic reactions [23] resulting in non-specific enzyme inhibitors; and, hopefully, an OA analog would preferentially inhibit *Mt*OPRT enzyme activity thereby minimizing undesirable side effects. In addition, as *Mt*OPRT follows an ordered kinetic mechanism (Fig. 1B) with PRPP binding first, an OA analog should also bind to *Mt*OPRT:PRPP binary complex thereby overcoming any rescue of enzyme activity due to PRPP substrate accumulation and sequestering of free PRPP from the cellular pool in the form of *Mt*OPRT:PRPP:OA analog ternary complex, which could affect other essential metabolic pathways, as purine synthesis and mycobacterial cell wall synthesis [23]. The most promising compounds were then subjected to chemical modifications (Schemes 1 and 2), and measurements of *in vitro* inhibitory activity of these derivatives showed improved inhibitory effects.

2. Results

2.1. Synthesis

Compounds **5** and **6** (Table 1) were selected for further optimization. Although compound **2** displayed a better inhibitory

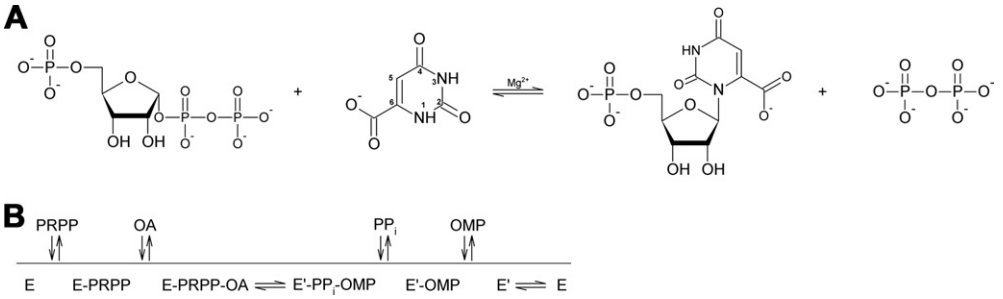

Fig. 1. (A) OPRT catalyzed conversion of OA and PRPP into OMP and PP_i by the formation of an *N*-glycosidic bond in the presence of Mg^{2+}. (B) Mono-Iso Ordered Bi Bi kinetic mechanism of *Mt*OPRT. E and E′ are different enzyme's isoforms. Adapted from Ref. [22].

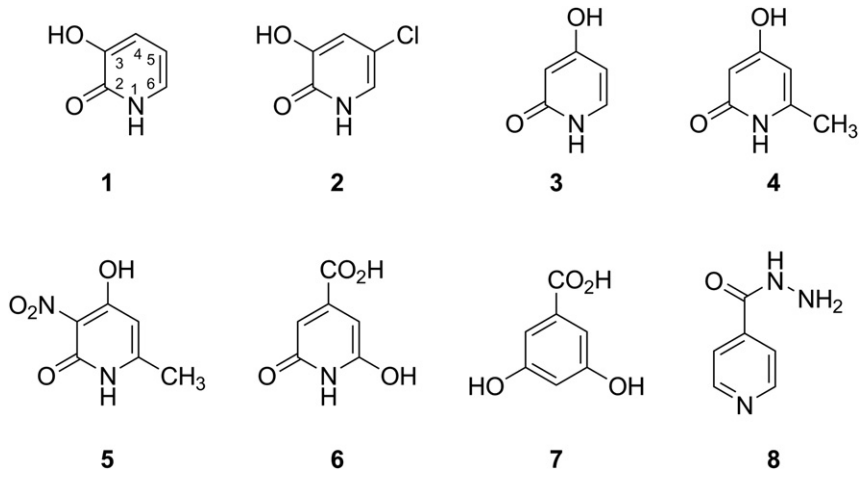

Fig. 2. Commercially available chemical compounds tested *in vitro* as possible *Mt*OPRT inhibitors.

profile (18%) as compared to **5** (15%), we favored **5** over **2** since the former presents the nucleophilic 5-position unoccupied, an important feature for our initial strategy of introducing amino alcohol derivatives as side chains in pyridine-2(1*H*)-one rings **5** and **6**. Acyclic mimics of the ribooxacarbenium ion of transition state analogues of purine nucleoside phosphorylases led to synthesis of inhibitory compounds with nanomolar dissociation constants [24]. We surmised that these amino alcohol derivatives would mimic the α-D-ribose leading to compounds more structurally similar to OMP product of *Mt*OPRT enzyme.

Compounds **9**–**12** were synthesized by classical Mannich reaction [25] with 63–95% yields (Scheme 1). The reactions were performed starting from **5** in the presence of amine or amino alcohol and paraformaldehyde using methanol as solvent. The reaction mixture was heated in sealed tubes at 100 °C for 2–16 h. All such compounds showed spectrometric properties corresponding to the proposed structures; and were then tested as potential inhibitors of *Mt*OPRT enzyme activity. None of these compounds showed better inhibitory activity as compared to the parent compound (Table 1). Our efforts were then directed at studying compound **6** and their derivatives.

The hydrophobic character of **6** was improved by condensation reaction of benzaldehydes in the presence of ethanol as solvent (Scheme 2). The reactions were conducted in reflux for 16–24 h furnishing the compounds **13**–**14** with 15–22% yields. These low yields can be attributed to formation of lactones derivatives in these reactions [26]. The Mannich reaction was also employed to obtain the amino and amino alcohol derivatives of **6** (Scheme 2). Likewise the reactions for synthesis of **9**–**12**, the compounds **15**–**16** were obtained by reaction of **6** and amino derivatives compounds in the presence of paraformaldehyde and methanol as solvent. The reaction mixtures were heated at 100 °C for 2–3 h leading to synthesis of the respective compounds with 43–48% yields (Scheme 2). In all performed attempts the dialkylated compound **16** was obtained as major product although the molar ratio was 1:1 pyridine-2(1*H*)-one **6** and dimethylamine. All synthesized compounds **13**–**16** showed spectrometric properties corresponding to the proposed structures.

2.2. Enzymatic activity assay and time-dependent inhibition

The reaction catalyzed by *Mt*OPRT 26 nM in the presence of saturated concentrations of both forward substrates was considered 100% under assay conditions. Initial inhibitory trials of compounds **1**–**8** indicated that compounds **1**, **3** and **4** did not show any effect on the reaction catalyzed by *Mt*OPRT at final concentrations of 100 μM (Fig. 2 and Table 1). The effect of addition of derivatives **9**–**16** at final concentrations of 100 μM in the

Table 1
Observed inhibitory activity, and inhibitory constants, of pyridinone-based compounds over *Mt*OPRT catalyzed reaction.

	Observed inhibitory activity[a]	K_{is} OA (μM)	Inhibition mode	K_{ii} PRPP (μM)	Inhibition mode
Commercially available compounds – initial screening					
1	None	–	–	–	–
2	18%	–	–	–	–
3	None	–	–	–	–
4	None	–	–	–	–
5	15%	–	–	–	–
6	90%	0.25 ± 0.03	Competitive	8.2 ± 0.4	Uncompetitive
7	15%	–	–	–	–
8	10%	–	–	–	–
Chemical derivatives					
9	2%	–	–	–	–
10	2.2%	–	–	–	–
11	7.5%	–	–	–	–
12	4%	–	–	–	–
13	95%	0.19 ± 0.01	Competitive	6.5 ± 0.2	Uncompetitive
14	60%	7.4 ± 0.6	Competitive	140 ± 9	Uncompetitive
15	71%	6.2 ± 0.4	Competitive	135 ± 7	Uncompetitive
16	40%	–	–	–	–

[a] Initial screening at 100 μM final concentration in the assay mixture.

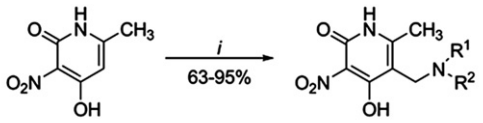

5 9-12

Entry	R^1	R^2	Time (h)	Yield (%)
9	CH_3	CH_3	2	95
10	H	CH_2CH_2OH	4	75
11	H	$CH_2CH(OH)CH_2OH$	16	63
12	H	$(CH_3)C(CH_2OH)CH_2OH$	8	82

Scheme 1.

cuvette was evaluated, showing that compounds **13**, **14** and **15** present inhibitory activities above 60% (Table 1), which was the cutoff here set to select inhibitors. However, only compound **13** showed better inhibitory activity than its parental molecule (Table 1). None of the selected compounds presented time-dependent inhibitory activity up to 30 min of pre-incubation with *Mt*OPRT (data not shown).

2.3. Inhibition assays

The mode of inhibition and inhibitor dissociation constants for compounds **6** and **13**–**15** are given in Table 1. These compounds showed competitive inhibition toward substrate OA (Figs. 3 and 4, A and C) as indicated by the pattern of intersecting lines that cross at the same value on the *y*-axis of the double reciprocal plots, suggesting that the binding of these inhibitors and OA are mutually exclusive. When substrate OA was fixed at saturating concentration and PRPP substrate concentration was varied in the presence of fixed-varying concentrations of **6** and **13**–**15**, these compounds showed a pattern of parallel lines in double reciprocal plots (Figs. 3 and 4 B and D). Accordingly, compounds **6** and **13**–**15** are uncompetitive inhibitors towards PRPP, suggesting both that these compounds do not bind to free enzyme form but bind to *Mt*OPRT:PRPP binary complex or subsequent species [27]. Fitting the competitive inhibition data to Eq. (1) and the uncompetitive inhibition data to Eq. (2) yielded the inhibitor dissociation constant values for compounds **6** and **13**–**15** presented in Table 1.

2.4. Isothermal titration calorimetry (ITC) binding assays

The best *Mt*OPRT inhibitors (**6** and its derivative **13**) were selected for further characterization of their binding mode by ITC. Binding assays conducted at 25 °C indicated that both molecules are able to bind to *Mt*OPRT:PRPP binary complex (Fig. 5). ITC data

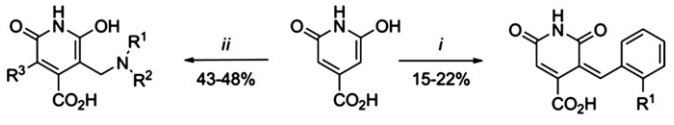

15-16 6 13-14

Entry	R^1	R^2	R^3	Yield (%)
13	H	--	--	22
14	OH	--	--	15
15	H	CH_2CH_2OH	H	43
16	CH_3	CH_3	$CH_2N(CH_3)_2$	48

Scheme 2.

were fitted to one set of sites binding model, yielding the thermodynamic constants ΔH and K_a. ΔS and ΔG values calculated from Eq. (3) and K_d as $1/K_a$. The number of ligand molecules bound per enzyme subunit (N) was directly derived from the one set of sites binding model, indicating that two molecules of inhibitor bind to biologically active homodimeric *Mt*OPRT (Fig. 5 and Table 2). Thermodynamic discrimination profiles indicate favorable enthalpic contribution ($-\Delta H$) for binding of compounds **6** and **13** to *Mt*OPRT:PRPP, and unfavorable entropy (positive $T\Delta S$) for **6** and favorable entropy (negative $T\Delta S$) for **13** (Table 2 and Fig. 6). In any case, the predominant contribution of ΔH resulted in favorable Gibbs energy ($-\Delta G$) for binding of both compounds (Table 2 and Fig. 6).

3. Discussion

Characterization of *Mt*OPRT [22] prompted us to propose, synthesize and test a few potential enzyme inhibitors. Accordingly, a series of derivatives (Schemes 1 and 2) of pyridine-2(1*H*)-one (Fig. 2) were synthesized and screened for *in vitro* inhibitory activity of *Mt*OPRT enzyme (Table 1). The mode of inhibition for the compounds that showed promising activity was evaluated (compounds **6** and **13**–**15**). In addition, the thermodynamic signatures of non-covalent interactions upon complex formation were evaluated for the two best inhibitors (**6** and **13**). Compounds **2**, **5**, **7** and **8** showed a slight inhibitory effect on *Mt*OPRT enzyme activity (Table 1).

It is noteworthy that inhibitory activity was increased by the presence of electron withdrawing groups attached at 3- and 5-position on the pyridine-2(1*H*)-one rings of compounds that were tested; where the compound 5-chloro-substituted **2** showed 18% of inhibitory activity whereas **1** showed no inhibitory activity (Table 1). The same pattern could be observed for compounds **4** and **5**, where 3-nitro substituted compound **5** at 100 μM showed 15% of inhibitory activity of *Mt*OPRT whereas compound **4** was ineffective in the same conditions (Table 1). The presence of these groups can increase the acidity of the hydrogen bound to the nitrogen of heterocyclic pyridine-2(1*H*)-one rings improving the putative interactions via hydrogen bonds with *Mt*OPRT active site. There also seems to be a need for the presence of the nitrogen (NH) in the pyridinone system for inhibitory activity, as compound **6** inhibitory activity (90%) is superior as compared to compound **7** (15%) both at 100 μM (Table 1). This result is in accordance with data from literature which showed that N1 of OA is involved in interactions with *Toxoplasma gondii* OPRT active site [18]. Interestingly, isoniazid (**8**), the most prescribed anti-tuberculosis drug [3,4], showed enzyme inhibitory activity of 10% at 100 μM final concentration (Table 1). This result is in agreement with the apparently promiscuous effect of isoniazid adducts on pyridine nucleotide-dependent dehydrogenases/reductases [28].

Compounds **13**–**16** are chemical derivatives of **6** (Scheme 2). Compound **13** showed better inhibitory activity (95%) than **14** (60%), suggesting that the presence of a hydroxyl group attached at 2-position of the phenyl substituent reduce the inhibitory activity (Table 1). Therefore, modest changes in analogue structure seem to cause relatively large changes in the ability to inhibit *Mt*OPRT activity. Compounds **15** and **16** showed inhibitory activity of, respectively, 71% and 40% (Table 1). Based on these data, the dialkylated compound **16** seems to display steric hindrance that could reduce its interaction with *Mt*OPRT. A threshold of 60% inhibitory activity of a specific compound was set as a starting point to carry out detailed determination of the mode of inhibition. Accordingly, compounds **6**, **13**–**15** (Table 1) were selected for further studies. None of these compounds presented time-dependent inhibition, which was assessed by measuring *Mt*OPRT enzyme activity as

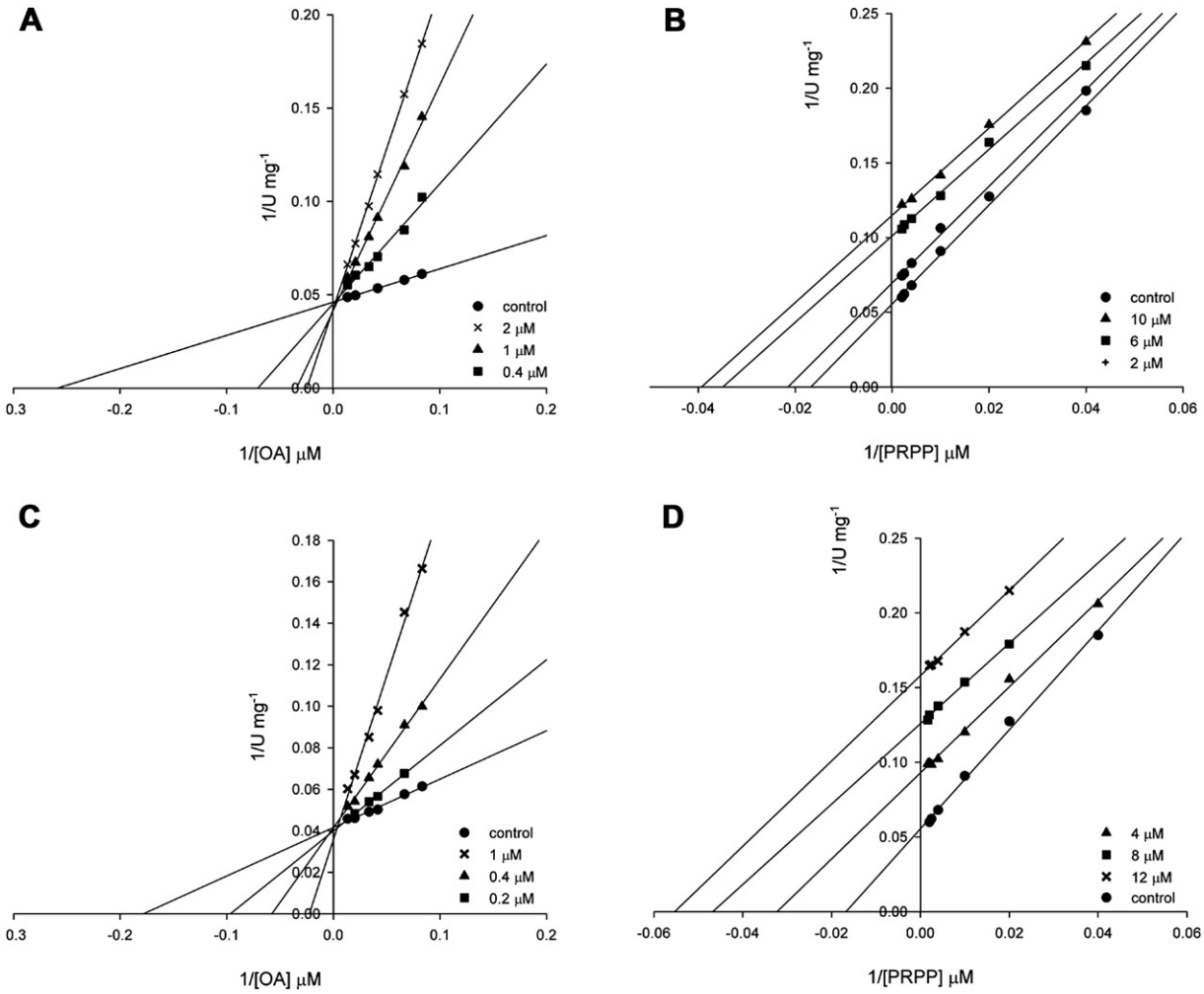

Fig. 3. Double-reciprocal plots of inhibition assays for compounds **6** (A, B) and **13** (C, D). Pattern of intersecting lines at *y*-axis are prognostic of competitive inhibition towards OA, whereas parallel lines indicate uncompetitive inhibition towards PRPP. Substrate OA was varied from 12 to 75 μM in presence of PRPP 500 μM (A, C), substrate PRPP was varied from 25 to 500 μM in presence of OA 50 μM (B, D). Each inhibitor variation range is depicted in the plots.

a function of time (up to 30 min) for enzyme pre-incubated with either compound **6**, **13**, **14** or **15** (*data not show*).

Inhibition assays for **6**, **13**–**15** showed that these compounds are competitive inhibitors with respect to OA substrate (Figs. 3 and 4, A and C). Accordingly, compounds **6**, **13**–**15** compete with OA for binding to *Mt*OPRT enzyme, as anticipated for structural mimics of OA substrate [27]. On the other hand, compounds **6**, **13**–**15** displayed uncompetitive inhibition with respect to PRPP substrate (Figs. 3 and 4, C and D). These data suggest that these compounds bind to *Mt*OPRT:PRPP, which is in agreement with *Mt*OPRT Mono–Iso Ordered Bi Bi kinetic mechanism (Fig. 1B). Hence, as compounds **6**, **13**–**15** are OA analogs and binding of PRPP must precede OA binding, compounds **6**, **13**–**15** compete with OA for molecular interactions with the *Mt*OPRT:PRPP binary complex. On the other hand, as PRPP binding is followed by OA, compounds **6**, **13**–**15** behave as uncompetitive inhibitors with respect to PRPP, showing increased binding to increasing concentrations of *Mt*OPRT:PRPP binary complex as PRPP concentration rises, and subsequent competitive inhibition towards OA binding to the binary complex.

As compounds **14** and **15** did not show increased inhibitory activity when compared to their parent molecule (**6**), binding of lead-like compounds **6** and **13** to *Mt*OPRT were characterized by ITC assays. Since compounds **6** and **13** are uncompetitive inhibitors with respect to PRPP, all ITC binding assays were carried out by titration of each inhibitor into a solution containing *Mt*OPRT enzyme incubated with PRPP 500 μM (5 times its K_m) and $MgCl_2$ 20 mM. $MgCl_2$ was included in the reaction mixture as the true substrate for *Mt*OPRT, as well as type I PRTases, is Mg^{2+}–PRPP complex [29]. ITC binding assays of compounds **6** and **13** in the absence of either PRPP or $MgCl_2$ indicated that inhibitor concentrations 10 times larger (for instance, compound **6** at 4 mM concentration) than in the presence of Mg^{2+}–PRPP complex yielded minor 1 kcal/mol variation (data not shown). ITC data obtained under these conditions could be an indicative that under a situation where inhibitor molecules accumulate to a significantly high intracellular concentration, they may bind to *Mt*OPRT free enzyme thereby overriding the enzyme kinetic mechanism. Any relevance of these data to intracellular physiological context remains to be tested though.

The ITC data (Fig. 5) were fitted to one set of sites binding model, indicating that there is no difference in binding affinity between the two active sites of the *Mt*OPRT homodimer. Thermodynamic data indicate a predominantly favorable (negative) enthalpy (ΔH) and favorable Gibbs free energy (ΔG) upon binding of both compounds to *Mt*OPRT:PRPP (Table 2 and Fig. 6). Taken together, these data are indicative that binding of compounds **6** and **13** to *Mt*OPRT are favorable spontaneous processes mainly ruled by

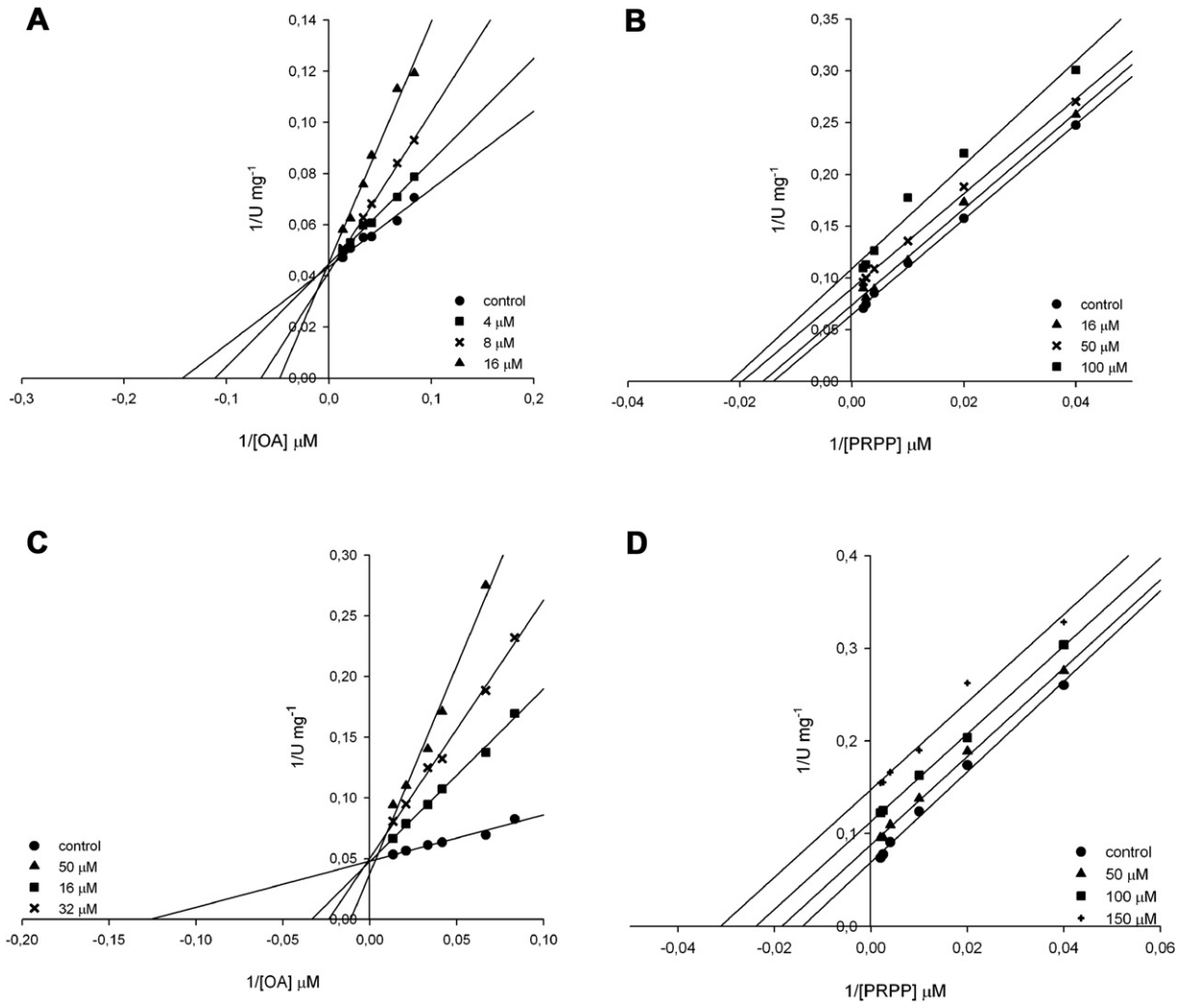

Fig. 4. Double-reciprocal plots of inhibition assays for compounds **14** (A, B) and **15** (C, D). Variation of substrate OA (A, C), and of substrate PRPP (B, D) were in the same range as for compounds **6** and **13** inhibition assays. Each inhibitor variation range is depicted in the plots.

formation of favorable hydrogen bonds and/or van der Waals interactions. The favorable entropic contribution (negative $T\Delta S$) of compound **13** binding may be accounted for by release of "bound" water molecules to bulk solvent. On the other hand, the unfavorable entropic contribution (positive $T\Delta S$) for compound **6** implies conformational changes upon *Mt*OPRT:PRPP:**6** ternary complex formation [30]. Although these conformational changes may be either in the enzyme or inhibitor, it is tempting to suggest that it corresponds to protein isomerization step upon ligand binding, which is a hallmark of enzymes that follow Iso Mechanisms [31]. It has been reported that movements of a catalytic flexible loop are integral to catalysis of phosphoribosyltransferase enzymes [29], allowing closing of active site, recruitment of catalytic essential residues, and displacement of water molecules to bulk solvent [32]. Binding of OMP product to *Mt*OPRT displays similar thermodynamic discrimination profile (Fig. 6), which could be explained by nearly complete conservation of OA moiety of OMP in compound **6**, except N1 (pyridine ring in **6**, pyrimidine ring in OA and OMP). It is thus tempting to suggest that compounds **6** and **13** can make key enzyme-ligand contacts in *Mt*OPRT active site involving N1, C2 and C6 ketone groups, in agreement with the three-dimensional structures of *Saccharomyces cerevisiae* OPRT in complex with ligands [33–35] and *T. gondii* OPRT [18].

Interestingly, the overall dissociation constant values (K_d; Table 2) for **6** (0.14 μM) and **13** (0.09 μM) are in fairly good agreement with the dissociation constant values (K_{is}; Table 1) for competitive inhibition with respect to OA substrate (0.25 μM for **6**, 0.19 μM for **13**). Interestingly, although compounds **6** and **13** binding processes showed a favorable enthalpic contribution, only compound **13** displayed favorable entropic contribution (Table 2). The latter may be attributed to release of solvation water molecules of the exocyclic aromatic ring substituent of **13** not present in **6**. It is thus tempting to suggest that the lower K_{is} and K_{ii} values for **13** (Table 1) are due to entropy optimization by increasing hydrophobicity, which results in larger log P (0.714 for **6**, and 0.938 for **13**) and log D (−3.92 for **6** and -2.58 for **13**) values at pH 8.0 for **13**. A general guide for optimal gastrointestinal absorption by passive diffusion permeability after oral dosing is to have a moderate log P (range 0–3), a requirement that is fulfilled by these compounds. Enthalpy and entropy simultaneous optimization is one of the major goals in drug discovery, which is not trivial due to enthalpy/entropy compensation [35]. The ITC data suggest that this goal was partially achieved for compound **13** as it retained the favorable enthalpic contribution of compound **6** binding to *Mt*OPRT:PRPP, and the unfavorable entropic contribution of **6** was converted into a favorable entropic contribution for **13** binding process (Table 2 and Fig. 6).

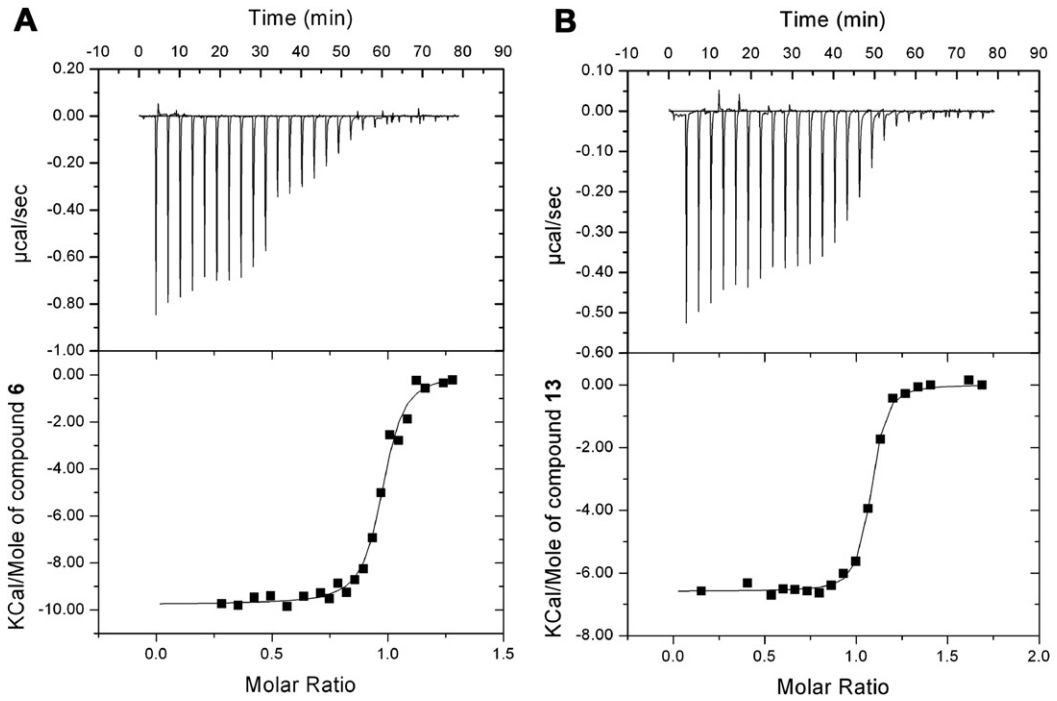

Fig. 5. ITC ligand binding assays. Binding isotherms of **6** (A) and **13** (B) were fitted to sequential binding sites model.

4. Conclusion

The favorable enthalpic and entropic contributions of molecule **13** binding to *Mt*OPRT:PRPP correspond to favorable thermodynamic profiles for high affinity ligands [36]. Taken together, the data here presented suggest that more potent *Mt*OPRT inhibitors may rely on optimization of compounds **6** and **13**, including exploration of lipophilicity that should address its effect on properties such as solubility, permeability and equilibrium inhibition constants, to name a few [37]. Interestingly, 2-aminosubstituted pyrimidine 5-carboxylate derivatives have been shown to be promising antitubercular lead molecules, even though their MIC values were larger than the isoniazid MIC [38]. As the *de novo* pyrimidine biosynthesis pathway has been shown to be required for cell invasion and virulence of obligatory parasites as *T. gondii* [12] and *Plasmodium vivax* [13], *Mt*OPRT may represent a target for the development of drugs to be used in TB treatment and prophylaxis [14]. Efforts to determine *in vivo* inhibitory effects of compounds **6** and **13** are currently underway. The results here presented may be useful to chemical biologists interested in designing loss-of-function (inhibitors) or gain-of-function (activators) chemical compounds to reveal the biological role of *Mt*OPRT in the context of whole MTB cells.

5. Experimental section

5.1. Synthesis – apparatus and analysis

Unless otherwise indicated, all common reactants and solvents were used as obtained from commercial suppliers without further purification. All melting points were measured using a Microquímica MQAPF-302 apparatus. ^{1}H NMR spectra were acquired on a Bruker DPX 400 (Federal University of Santa Maria, UFSM/Brazil) or Anasazi EFT-60 spectrometer (^{1}H at 400.13 MHz or 60.13 MHz, respectively) at 25 °C, for DPX 400, and 30 °C for EFT-60, in 5 mm sample tubes. DMSO-d_6 was used as solvent and TMS was used as internal standard. High resolution mass spectra were obtained for all compounds on a LTQ Orbitrap Discovery mass spectrometer (Thermo Fisher Scientific). This hybrid system meets the LTQ XL linear ion trap mass spectrometer and an Orbitrap mass analyzer. The experiments were performed via direct infusion of sample in MeOH 50%/FA 0.1% (flow: 5 µL min^{-1}) in the positive-ion mode using electrospray ionization. Elemental composition calculations were executed using the specific tool included in the Qual Browser module of Xcalibur (Thermo Fisher Scientific, release 2.0.7) software. Fourier transform infrared (FTIR) spectra were recorded using a universal attenuated total reflectance (UATR) attachment on a PerkinElmer Spectrum 100 spectrometer in the wavenumber range of 650–4000 cm^{-1} with resolution of 4 cm^{-1}. All TLC analyses were performed on silica gel 0.2 mm (Aldrich 60 F254) and spots revealed by UV visualization at 360 nm.

5.2. General procedure for the synthesis of pyridine-2(1H)-one *9–12*

The mixture of 4-Hydroxy-6-methyl-3-nitropyridin-2(1*H*)-one **5** (1.0 mmol, 0.170 g), amine or amino alcohol (1.0 mmol) and paraformaldehyde (0.030 g) in methanol (10 mL) was heated in a sealed tube at 100 °C for the appropriate time (Scheme 1). After cooling to room temperature the solvent was evaporated under reduced pressure. The solid obtained was washed with distilled water

Table 2
Thermodynamic functions and number of ligands per subunit (*N*) for binding of compounds **6** and **13** to *Mt*OPRT:PRPP binary complex.

Compound	ΔH (cal/mol)	$-T\Delta S$ (cal/mol/deg)	ΔG (cal/mol)	K_a (M^{-1})	K_d (µM)	*N*
6	$-9.8 \pm 0.1 \times 10^3$	390 ± 6	$-9.4 \pm 0.1 \times 10^3$	$7 \pm 1 \times 10^6$	0.14 ± 0.03	0.932 ± 0.005
13	$-6.6 \pm 0.1 \times 10^3$	$-3.04 \pm 0.02 \times 10^3$	$-9.63 \pm 0.07 \times 10^3$	$12 \pm 2 \times 10^6$	0.09 ± 0.01	1.05 ± 0.03

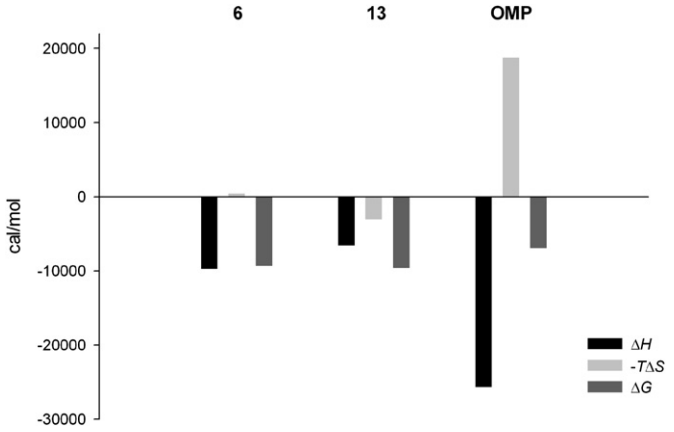

Fig. 6. Enthalpy (ΔH), entropy ($-T\Delta S$) and Gibbs free energy (ΔG) thermodynamic profile for **6**, **13** and substrate OMP binding to *Mt*OPRT. ITC data for OMP binding was previously described elsewhere (in press, Molecular BioSystems, doi:10.1039/C1MB05402C) and is given here for comparison only.

(3 × 10 mL) and cold hexane (2 × 10 mL). When necessary, the products were recrystallized from 10% EtOAc in hexane, yielding the analytically pure pyridine-2(1*H*)-ones **9**–**12**. After, the products were dried under reduced pressure at 38 °C for at least 24 h.

5.2.1. 5-((Dimethylamino)methyl)-4-hydroxy-6-methyl-3-nitropyridin-2(1H)-one (**9**)

Yellow powder; yield: 0.216 g (95%); M.p. 143–145 °C; ^{1}H NMR (60 MHz, DMSO-d_6): δ 2.03 (s, 3H, CH_3), 2.65 (s, 6H, $N(CH_3)_2$), 3.81 (s, 2H, CH_2), 11.01 (br, 1H, NH); FTIR (UATR, cm^{-1}): 3041, 2817, 1629, 1533, 1403, 1274, 1167, 793; HRMS (ESI) calcd for $C_9H_{13}N_3O_4$ + H: 228.0979. Found 228.0981 $(M + H)^+$.

5.2.2. 4-Hydroxy-5-((2-hydroxyethylamino)methyl)-6-methyl-3-nitropyridin-2(1H)-one (**10**)

Yellow powder; yield: 0.182 g (75%); M.p. 139–141 °C; ^{1}H NMR (400 MHz, DMSO-d_6): δ 2.16 (s, 3H, CH_3), 2.94 (t, 2H, CH_2), 3.45 (t, 2H, CH_2), 3.88 (s, 2H, CH_2), 8.00 (br, 2H), 10.09 (br, 1H, NH); FTIR (UATR, cm^{-1}): 3379, 3158, 2954, 2803, 1609, 1529, 1416, 1266, 1190, 1068, 803, 788; HRMS (ESI) calcd for $C_9H_{13}N_3O_5$ + H: 244.0928. Found 244.0929 $(M + H)^+$.

5.2.3. 5-((2,3-Dihydroxypropylamino)methyl)-4-hydroxy-6-methyl-3-nitropyridin-2(1H)-one (**11**)

Light yellow powder; yield: 0.172 g (63%); M.p. 109–111 °C; ^{1}H NMR (400 MHz, DMSO-d_6): δ 2.06 (s, 3H, CH_3), 2.78–2.81 (dd, 2H, CH_2), 3.03–3.07 (m, 1H, CH), 3.42–3.45 (dd, 2H, CH_2), 3.86 (s, 2H, CH_2), 5.33 (br, 2H), 10.02 (br, 2H); FTIR (UATR, cm^{-1}): 3235, 3004, 2806, 1638, 1518, 1435, 1252, 1187, 1035, 776; HRMS (ESI) calcd for $C_{10}H_{15}N_3O_6$ + H: 274.1034. Found 274.1039 $(M + H)^+$.

5.2.4. 5-((1,3-Dihydroxy-2-methylpropan-2-ylamino)methyl)-4-hydroxy-6-methyl-3-nitropyridin-2(1H)-one (**12**)

Yellow powder; yield: 0.235 g (82%); M.p. 91–93 °C; ^{1}H NMR (400 MHz, DMSO-d_6): δ 1.35 (s, 3H, CH_3), 2.10 (s, 3H, CH_3), 3.32 (s, 4H, $2CH_2$), 3.91 (s, 2H, CH_2), 10.01 (br, 1H, NH); FTIR (UATR, cm^{-1}): 3167, 2941, 1610, 1515, 1399, 1268, 1178, 1055, 824, 787; HRMS (ESI) calcd for $C_{11}H_{17}N_3O_6$ + H: 288.1190. Found 288.1204 $(M + H)^+$.

5.3. General procedure for the synthesis of pyridine-2(1H)-one **13**–**14**

The mixture of 2,6-Dihydroxypyridine-4-carboxylic acid **6** (1.0 mmol, 0.155 g) and aldehyde (1.0 mmol) was stirred under reflux in dry ethanol (10 mL) for 16 h, compound **13**, and 24 h for **14**. The progress of the reaction was monitored by TLC using a solution of EtOAc and hexane (1:1, v/v) as a mobile phase. After cooling to room temperature the solid formed was filtered and washed with distilled water (2 × 10 mL) and Et_2O (2 × 10 mL). The products were recrystallized from hexane and dried under reduced pressure at 38 °C for 24 h.

5.3.1. 3-Benzylidene-2,6-dioxo-1,2,3,6-tetrahydropyridine-4-carboxylic acid (**13**)

Pale yellow powder; yield: 0.053 g (22%); M.p. 254–258 °C (Dec); ^{1}H NMR (60 MHz, DMSO-d_6): δ 6.46 (s, 1H, CH), 7.09–7.22 (m, 5H, Ph), 7.35 (s, 1H, CH); FTIR (UATR, cm^{-1}): 3073, 1669, 1572, 1480, 1465, 1221, 758; HRMS (ESI) calcd for $C_{13}H_9NO_4$ + H: 244.0604. Found 244.0603 $(M + H)^+$.

5.3.2. 3-(2-Hydroxybenzylidene)-2,6-dioxo-1,2,3,6-tetrahydropyridine-4-carboxylic acid (**14**)

Beige powder; yield: 0.039 g (15%); M.p. 232–234 °C; ^{1}H NMR (60 MHz, DMSO-d_6): δ 6.48 (s, 1H, CH), 6.98–7.37 (m, 4H, C_6H_5), 7.45 (s, 1H, CH); FTIR (UATR, cm^{-1}): 3069, 1666, 1568, 1486, 1455, 1224, 752; HRMS (ESI) calcd for $C_{11}H_{17}N_3O_6$ + H: 288.1190. Found 288.1204 $(M + H)^+$.

5.4. General procedure for the synthesis of pyridine-2(1H)-one **15**–**16**

The mixture of 2,6-Dihydroxypyridine-4-carboxylic acid **6** (1.0 mmol, 0.155 g), amine or amino alcohol (1.0 mmol) and paraformaldehyde (0.030 g) in methanol (10 mL) was heated in a sealed tube at 100 °C for 3 h, compound **15**, and 2 h for **16**. After cooling to room temperature the solvent was evaporated under reduced pressure. The solid obtained was diluted in distilled water (20 mL) and filtered (0.22 μm). After, the water was evaporated under reduced pressure. Finally, the product was washed with cold hexane (2 × 10 mL) and dried under reduced pressure at 30 °C for 24 h.

5.4.1. 6-Hydroxy-5-((2-hydroxyethylamino)methyl)-2-oxo-1,2-dihydropyridine-4-carboxylic acid (**15**)

Dark-red solid; yield: 0.098 g (43%); M.p. 48–50 °C; ^{1}H NMR (400 MHz, DMSO-d_6): δ 2.81 (t, 2H, CH_2), 3.55 (t, 2H, CH_2), 3.68 (s, 2H, CH_2), 5.19 (br, 2H), 6.53 (s, 1H, CH); FTIR (UATR, cm^{-1}): 2843, 1561, 1450, 1411, 1327, 1176, 1078, 991, 763; HRMS (ESI) calcd for $C_9H_{12}N_2O_5$ + H: 229.0819. Found 229.0816 $(M + H)^+$.

5.4.2. 3,5-Bis((dimethylamino)methyl)-6-hydroxy-2-oxo-1,2-dihydropyridine-4-carboxylic acid (**16**)

Black solid; yield: 0.131 g (48%); M.p. 101–103 °C; ^{1}H NMR (60 MHz, DMSO-d_6): δ 2.70 (s, 9H, $2N(CH_3)_2$), 3.98 (s, 2H, CH_2); FTIR (UATR, cm^{-1}): 3052, 2802, 1583, 1465, 1357, 1299, 1022, 759; HRMS (ESI) calcd for $C_{12}H_{19}N_3O_4$ + H: 270.1448. Found 270.1442 $(M + H)^+$.

5.5. Enzymatic activity assay

All chemicals were purchased from Sigma Aldrich. Homogeneous recombinant *Mt*OPRT was obtained as previously described [22]. Effect of each compound on *Mt*OPRT activity was measured for the forward phosphoribosyltransferase reaction ($OA + PRPP \rightarrow OMP + PP_i$) by monitoring the decrease in OA concentration. The assay was performed in quartz cuvettes with UV–visible Shimadzu spectrophotometer UV2550 equipped with a temperature-controlled cuvette holder. The reaction mixture (500 μL) contained Tris HCl 50 mM $MgCl_2$ 20 mM pH 8.0, OA 50 μM, PRPP 500 μM and *Mt*OPRT 26 nM. Reaction was started by the

addition of enzyme, and a linear progress curve of absorbance change at 295 nm by 60 s at 25 °C was followed. The extinction coefficient of this conversion was 3950 M^{-1} cm^{-1} [39]. Inhibitors were then added to reaction mixture at final concentration of 100 μM and enzyme activity was measured as before. All enzymatic activity and further assays were performed in duplicate or triplicate. Selection of inhibitors for further assays was based on the difference of enzyme activity in absence and presence of inhibitor 100 μM, and a cutoff was set to a 60% inhibitory activity.

5.6. Time-dependent inhibition

Evaluation of time-dependent inhibitory activity was evaluated at the same enzymatic assay conditions as described above. Aliquots corresponding to 26 nM of *Mt*OPRT were taken at different times (up to 30 min) from pre-incubation mixtures containing *Mt*OPRT and inhibitor at final concentration of 1 μM. These aliquots were added to a reaction mixture containing OA 50 μM, PRPP 500 μM, and OA → OMP conversion under steady-state conditions was monitored as a linear decrease in absorbance at 295 nm.

5.7. Inhibition assays

Inhibition assays were carried out in 500 μL of reaction mixtures containing Tris HCl 50 mM $MgCl_2$ 20 mM, 26 nM *Mt*OPRT, at 25 °C, monitoring disappearance of OA at 295 nm for 60 s. In the inhibition assays one substrate concentration was constant at saturating level (5 times its K_m value, OA = 50 μM and PRPP = 500 μM) whereas the second substrate was varied (PRPP: 25–500 μM, OA: 12–75 μM), in absence and presence of varied concentrations of each inhibitor (**6**: 0.4–10 μM, **13**: 0.2–12 μM, **14**: 4–100 μM, **15**: 16–150 μM). Double reciprocal data were fitted to Eq. (1)

$$v = VA/[K(1 + I/K_{is}) + A] \quad (1)$$

or Eq. (2)

$$v = VA/[A(1 + I/K_{ii}) + K], \quad (2)$$

which describe, respectively, competitive and uncompetitive inhibition mechanisms. In these equations, *v*, *V*, *A*, and *I* correspond to, respectively, the steady-state reaction rate, maximum reaction rate, substrate *A* concentration, and inhibitor *I* concentration; and *K* is the Michaelis–Menten constant (K_m) for the varied substrate, K_{is} is the dissociation constant of inhibitor *I* for competitive inhibition, and K_{ii} is the dissociation constant of inhibitor *I* for uncompetitive inhibition. All data were evaluated using SigmaPlot version 11.0 software (Systat Software, Inc., San Jose California USA). All measurements were performed in duplicate or triplicate with at least five varied substrate and inhibitor concentrations.

5.8. ITC binding assays

Binding of inhibitors (**6** and **13**) to *Mt*OPRT:PRPP were evaluated by ITC using an iTC_{200} Microcalorimeter (Microcal, Inc., Northampton, MA). Reference cell (200 μL) was loaded with Milli-Q water for all assays. The injection syringe (39.7 μL) was filled with inhibitors **6** and **13** at 400 μM concentration. Ligand binding isotherms were measured by direct titration (ligand into macromolecule). Titration first injection (0.5 μL) was not used in data analysis and was followed by 13 injections of 2.26 μL plus 12 injections of 1.13 μL each, spaced by 180 s, into *Mt*OPRT 60 μM incubated with PRPP 500 μM in an assay mixture containing $MgCl_2$ 20 mM (sample cell) in buffer Gly–Gly 100 mM pH 8.0. Buffer Gly–Gly 100 mM replaced Tris HCl 50 mM due to high enthalpy of ionization of the latter [40]. Control titrations (ligand into buffer) were performed to subtract the heats of dilution and mixing for each experiment prior to data analysis. ITC data were fitted to Eq. (3),

$$\Delta G = \Delta H - T\Delta S = RT\ln K_a, \quad (3)$$

in which ΔH represents the enthalpy change, ΔG the Gibbs free energy change, ΔS the entropy change, *T* the temperature of the experiment in Kelvin, R the gas constant (1.987 cal K^{-1} mol^{-1}), and K_a the equilibrium association constant. The equilibrium dissociation constant, K_d, was calculated by the inverse of K_a. All data were evaluated utilizing the Origin 7 SR4 software (Microcal, Inc., Northampton, MA). Entropy values are presented as $-T\Delta S$.

Acknowledgments

This work was supported by funds of National Institute of Science and Technology on Tuberculosis (INCT-TB), MCT-CNPq, Ministry of Health – Department of Science and Technology (DECIT) – Secretary of Health Policy (Brazil) to D.S.S. and L.A.B. L.A.B. and D.S.S. also acknowledge financial support awarded by FAPERGS-CNPq-PRONEX-2009. A.A.S (CNPq 306764/2010-5), L.A.B. (CNPq, 520182/99-5) and D.S.S. (CNPq, 304051/1975-06) are Research Career Awardees of the National Research Council of Brazil (CNPq). A.B. acknowledges scholarship awarded by BNDES. P.M. and L.A.R. acknowledge scholarships awarded by CNPq.

References

[1] T.R. Rustad, A. Sherrid, K. Minch, D. Sherman, Hypoxia: a window into *Mycobacterium tuberculosis* latency, Cell. Microbiol. 11 (2009) 1151–1159.
[2] R.G. Ducati, A. Ruffino-Netto, L.A. Basso, D.S. Santos, The resumption of consumption: a review on tuberculosis, Mem. Instit. Oswaldo Cruz 7 (2006) 697–714.
[3] World Health Organization, Global Tuberculosis Control – Epidemiology, Strategy, Financing Available from: (2009) www.who.int/tb/publications/global_report/2009.
[4] Z. Ma, C. Lienhardt, H. McIlleron, A. Nunn, X. Wang, Global tuberculosis drug development pipeline: the need and the reality, Lancet 375 (2010) 2100–2109.
[5] R. Zaleskis, Adverse effects of anti-tuberculosis chemotherapy, Eur. Respir. Dis. (2006) 47–49.
[6] D.G. Russell, C.E. Barry 3rd, J.A.L. Flynn, Tuberculosis: what we don't know can, and does, hurt us, Science 328 (2010) 852–856.
[7] A.A. Velayati, P. Farnia, M.R. Masjedi, T.A. Ibrahim, P. Tabarsi, R.Z. Haroun, H.O. Kuan, J. Ghanavi, P. Farnia, M. Varahram, Totally drug-resistant tuberculosis strains: evidence of adaptation at the cellular level, Eur. Respir. J. 34 (2009) 1202–1203.
[8] A.A. Velayati, M.R. Masjedi, P. Farnia, P. Tabarsi, J. Ghanavi, A.H. ZiaZarifi, S.E. Hoffner, Emergence of new forms of totally drug-resistant tuberculosis bacilli, Chest 136 (2009) 420–425.
[9] J.E. Gomez, J.D. MdKinney, *M. Tuberculosis* persistence, latency, and drug tolerance, Tuberculosis (Edinb) 84 (2004) 29–44.
[10] S. Hasan, S. Daugelat, P.S. Srinivasa-Rao, M. Schreiber, Prioritizing genomic drug targets in pathogens: application to *Mycobacterium tuberculosis*, PLoS Comput. Biol. 2 (2006) e61.
[11] C.M. Sassetti, H.B. Dana, E.J. Rubin, Genes required for mycobacterial growth defined by high density mutagenesis, Mol. Microbiol. 48 (2003) 77–84.
[12] B.A. Fox, D.J. Bzik, *De novo* pyrimidine biosynthesis is required for virulence of *Toxoplasma gondii*, Nature 415 (2002) 926–930.
[13] S.R. Krungkrai, S. Aoki, N.M.Q. Palacpac, D. Sato, T. Mitamura, J. Krungkrai, T. Horii, Human malaria parasite orotate phosphoribosyltransferase: functional expression, characterization of kinetic reaction mechanism and inhibition profile, Mol. Biochem. Parasitol. 134 (2004) 245–255.
[14] H.I.M. Boshoff, C.E. Barry 3rd, Tuberculosis – metabolism and respiration in the absence of growth, Nat. Rev. Microbiol. 3 (2005) 70–80.
[15] Y. Zhang, V.L. Schramm, Pyrophosphate interactions at the transition states of *Plasmodium falciparum* and human orotate phosphoribosyltransferases, J. Am. Chem. Soc. 132 (2010) 8787–8794.
[16] M. Abdo, Y. Zhang, V.L. Schramm, S. Knapp, Electrophilic aromatic selenylation: new OPRT inhibitors, Org. Lett. 12 (2010) 2982–2985.
[17] Y. Zhang, M. Luo, V.L. Schramm, Transition states of *Plasmodium falciparum* and human orotate phosphoribosyltransferases, J. Am. Chem. Soc. 131 (2009) 4685–4694.
[18] Z.Z. Javaid, M.H. el Kouni, M.H. Ilzsch, Pyrimidine nucleobase ligands of orotate phosphoribosyltransferase from *Toxoplasma gondii*, Biochem. Pharmacol. 58 (1999) 1457–1465.

[19] O.H. Temmink, M. Bruin, A. Turksma, S. Cricca, A. Laan, G. Peters, Activity and substrate specificity of pyrimidine phosphorylases and their role in fluoropyrimidine sensitivity in colon cancer cell lines, Int. J. Biochem. Cell Biol. 39 (2007) 565–575.
[20] W. Ichikawa, Prediction of clinical outcome of fluoropyrimidine-based chemotherapy for gastric cancer patients, in terms of the 5-fluoruracil metabolic pathway, Gastric Cancer 9 (2006) 145–155.
[21] J.F. Witte, K.E. Bray, C.K. Thornburg, R.W. McClard, 'Irreversible' slow-onset inhibition of orotate phosphoribosyltransferase by an amidrazone phosphate transition-state mimic, Bioorg. Med. Chem. Lett. 16 (2006) 6112–6115.
[22] A. Breda, L.A. Rosado, D.M. Lorenzini, L.A. Basso, D.S. Santos, Molecular, kinetic and thermodynamic characterization of *Mycobacterium tuberculosis* orotate phosphoribosyltransferase, Mol. BioSyst. 5 (2012) 572–586.
[23] A.P. Lucarelli, S. Buroni, M.R. Pasca, M. Rizzi, A. Cavagnino, G. Valentini, G. Riccardi, L.R. Chiarelli, *Mycobacterium tuberculosis* phosphoribosylpyrophosphate synthetase: biochemical features of a crucial enzyme for mycobacterial cell wall biosynthesis, PLoS ONE 5 (2010) e15494.
[24] E.A. Taylor, K. Clinch, P.M. Kelly, L. Li, G.B. Evans, P.C. Tyler, V.L. Schramm, Acyclic ribooxacarbenium ion mimics as transition state analogues of human and malarial purine nucleoside phosphorylase, J. Am. Chem. Soc. 129 (2007) 6984–6985.
[25] C. Mannich, W. Krösche, Ueber ein kondensationsprodukt aus formaldehyd, ammoniak und antipyrin, Archiv Der Pharmazie 250 (1912) 647–667.
[26] R.H. Wiley, H. Kraus, 3-Arylidene-5-(α-hydroxybenzylidene)-2,6-piperidinedione-4-carboxylic acid γ-lactones from citrazinic acid, J. Org. Chem. 21 (1956) 757–758.
[27] R.A. Copeland, Evaluation of Enzyme Inhibitors in Drug Discovery, first ed. John Wiley & Sons, 2005.
[28] A. Argyrou, L. Jin, L. Siconilfi-Baez, R.H. Angeletti, J.S. Blanchard, Proteome-wide profiling of isoniazid targets in *mycobacterium tuberculosis*, Biochemistry 45 (2006) 13947–13953.
[29] S.C. Sinha, J.L. Smith, The PRT protein family, Curr. Opin. Struct. Biol. 11 (2001) 733–739.
[30] R. O'Brien, I. Haq, Applications of biocalorimetry: binding, stability and enzyme kinetics, in: J.E. Ladbury, M.L. Doyle (Eds.), Biocalorimetry 2 Applications of Calorimetry in the Biological Sciences, John Wiley & Sons, 2004, pp. 3–34.
[31] K.L. Rebholz, D.B. Northrop, Kinetics of iso mechanisms, Methods Enzymol. 249 (1995) 211–239.
[32] G.P. Wang, C. Lundegaard, K.F. Jensen, C. Grubmeyer, Kinetic mechanism of OMP synthase: a slow physical step following group transfer limits catalytic rate, Biochemistry 38 (1999) 275–283.
[33] G. Scapin, C. Grubmeyer, J.C. Sacchetinni, Crystal structure of orotate phosphoribosyltransferase, Biochemistry 33 (1994) 1287–1294.
[34] G. Scapin, D.H. Ozturk, C. Grubmeyer, J.C. Sacchetinni, The crystal structure of the orotate phosphoribosyltransferase complexed with orotate and α-D-5-phosphoribosyl-1-pyrophosphate, Biochemistry 34 (1995) 10744–10754.
[35] L. González-Segura, J.F. Witte, R.W. McClard, T.D. Hurley, Ternary complex formation and induced asymmetry in orotate phosphoribosyltransferase, Biochemistry 46 (2007) 14075–14086.
[36] E. Freire, Do enthalpy and entropy distinguish first in class from best in class? Drug Discov. Today 13 (2008) 869–874.
[37] E.H. Kerns, L. Di, Drug-like Properties: Concepts, Structure Design and Methods from ADME to Toxicity Optimization, first ed. Elsevier, San Diego, 2008.
[38] K. Singh, B. Wan, S. Franzblau, K. Chibale, J. Balzarini, Facile transformation of Biginelli pyrimidin-2(1*H*)-ones to pyrimidines. *In vitro* evaluation as inhibitors of *Mycobacterium tuberculosis* and modulators of cytostatic activity, Eur. J. Med. Chem. 46 (2011) 2290–2294.
[39] S.R. Krungkrai, B.J. Delfraino, J.A. Smiley, P. Prapunwattana, T. Mitamura, T. Horii, J. Krungkrai, A novel enzyme complex of orotate phosphoribosyltransferase and orotidine 5′-monophosphate decarboxylase in human malaria parasite *Plasmodium falciparum*: physical association, kinetics and inhibition characterization, Biochemistry 44 (2005) 1643–1652.
[40] H. Fukada, K. Takahashi, Enthalpy and heat capacity changes for the proton dissociation of various buffer components in 0.1 M potassium chloride, Proteins 33 (1998) 159–166.